2004

Widmanstatten ferrite plate formation in low-carbon steels

Dominic Phelan
University of Wollongong, phelan@uow.edu.au

Rian Dippenaar
University of Wollongong, rian@uow.edu.au

Recommended Citation

Widmanstatten ferrite plate formation in low-carbon steels

Abstract

The mechanism by which Widmanstätten ferrite plates nucleate and grow in low-carbon steels has been studied. In-situ laser scanning confocal microscopy (LSCM) observations, optical microscopy, and electron backscattered diffraction (EBSD) techniques have been used to characterize the relationship between grain boundary allotriomorphs and Widmanstätten ferrite plates. The issue of where Widmanstätten ferrite plates nucleate is one of some debate, with theories including morphological instability and sympathetic nucleation. Evidence has been found that supports the theory of a sympathetic nucleation mechanism being responsible for the formation of Widmanstätten ferrite plates. The EBSD measurements have shown that low-angle misorientations of between 5 and 10 deg exist between ferrite allotriomorphs and Widmanstätten ferrite plates.

Keywords

carbon, low, steels, formation, widmanstatten, plate, ferrite

Disciplines

Engineering | Science and Technology Studies

Publication Details

Widmanstätten Ferrite Plate Formation in Low-Carbon Steels

DOMINIC PHELAN and RIAN DIPPENAAR

The mechanism by which Widmanstätten ferrite plates nucleate and grow in low-carbon steels has been studied. *In-situ* laser scanning confocal microscopy (LSCM) observations, optical microscopy, and electron backscattered diffraction (EBSD) techniques have been used to characterize the relationship between grain boundary allotriomorphs and Widmanstätten ferrite plates. The issue of where Widmanstätten ferrite plates nucleate is one of some debate, with theories including morphological instability and sympathetic nucleation. Evidence has been found that supports the theory of a sympathetic nucleation mechanism being responsible for the formation of Widmanstätten ferrite plates. The EBSD measurements have shown that low-angle misorientations of between 5 and 10 deg exist between ferrite allotriomorphs and Widmanstätten ferrite plates.

I. INTRODUCTION

THE decomposition products of austenite have been systematically described by Dube *et al.,*[1] modified by Aaronson,[2] and reviewed by Dunne.[3] One of these decomposition products, Widmanstätten ferrite, has aroused some debate over the mechanism of both nucleation and growth. The nucleation of Widmanstätten ferrite has been attributed to either the propagation of an unstable interface or as a sympathetic nucleation event. Townsend and Kirkaldy[4] and Kirkaldy[5] have suggested that Widmanstätten ferrite plates form by the propagation of an unstable interface. Conversely, Aaronson *et al.*[6] proposed that a sympathetic nucleation mechanism is operative.

A. *Unstable Interface Mechanism*

Mullins and Sekerka[7,8] (M–S) developed a model of interface stability that incorporated both thermal and solute gradients and interfacial energy considerations. They were able to describe the conditions for the onset of a perturbed interface and the scale of such a perturbation for both liquid-solid and solid-solid phase transformations. Applying this analysis to austenite decomposition, Townsend and Kirkaldy[4] used quench-arrest-quench heat treatments, followed by sectioning and metallographic analysis, to study the kinetics and mechanism of Widmanstätten ferrite plate growth in iron-carbon alloys. They suggested that allotriomorphs displaying angular periodicy might be instabilities from which Widmanstätten plates propagate. Townsend and Kirkaldy concluded that Widmanstätten plate spacing is a function of M–S type instability.

B. *Sympathetic Nucleation*

The concept of sympathetic nucleation was introduced by Aaronson and Wells,[9] and critically reassessed by Aaronson *et al.*[6] Using the decomposition of austenite in iron-carbon alloys as an example, sympathetic nucleation is said to occur when a nucleus of alpha-ferrite forms at the interface between a pre-existing alpha-ferrite precipitate and the parent austenite phase. However, the conditions under which this nucleation mechanism could be thermodynamically favorable were not immediately apparent to Aaronson and Wells.[9] It was Shewmon's[10] critique of the application of the M–S analysis to solid-state phase transformations that provided a sound theoretical understanding of the conditions that would lead to sympathetic nucleation in general and, in the present context, specifically to the nucleation of Widmanstätten ferrite plates. It was recognized that despite the fact that perturbations may be predicted by the application of an M–S analysis, they are often not observed. Shewmon raised the point that strain energy and interfacial reaction kinetics play a role in stabilizing planar interfaces in solid-state phase transformations. These are not accounted for in the M–S analysis and it is for this reason that perturbations predicted by the M–S analysis are often not observed. Aaronson *et al.*[6] furthermore emphasized that if the interface between a pre-existing precipitate and the parent phase is incoherent, equilibrium solute concentration must exist at the interface. This can be reasoned because with incoherent interfaces, the inherent mobility of the interface is very high, and therefore, the rate of progression of such an interface is controlled by the diffusion of solute alone. Supersaturation of solute at the interface does not develop, and therefore, the Helmholtz volume free energy change required for the nucleation of a precipitate at the interface approaches zero. Consequently, the steady-state rate of sympathetic nucleation would also approach zero. Additionally, even if the driving force were high, any nuclei precipitating at an advancing austenite/alpha-ferrite interface would be over-run by the rapid progression of the incoherent interface before the nucleus would reach the critical radius that would allow further growth to occur.[6]

Shewmon[10] recognized that the conditions for nucleation are different if there is partial or full coherency between pre-existing alpha-ferrite and the parent phase, and equilibrium solute distribution will not exist at the interface. The immobility of the ledges of a coherent ferrite/austenite interface leads to solute diffusing away from the interface, resulting in supersaturation within the austenite and, hence, to an

increase in the chemical thermodynamic driving force for sympathetic nucleation. Evidence to support this concept is the presence of low-energy boundaries between the sympathetically nucleated crystal and the parent crystal, which was reported for Ti-Cr alloys by Menon and Aaronson,[11] in a duplex stainless steel by Ameyama *et al.*[12] and for proeutectoid ferrite sideplates and ferrite allotriomorphs by Spanos and Hall.[13]

In-situ observations of Widmanstätten ferrite plate growth in combination with crystallographic orientation analysis have, to the authors' knowledge, not been reported in the literature. In this study, observations were made, in real time, of the initial growth of Widmanstätten ferrite plates from allotriomorphs. These *in-situ* observations have been complemented by optical and electron backscattered diffraction analysis of the same regions to assess the nucleation mechanism by which Widmanstätten ferrite plates develop and propagate.

II. PROCEDURES

A low-carbon, silicon-killed steel, of composition listed in Table I, was used in this study. Samples were solution treated at a temperature of 1450 °C for 10 minutes in the single-phase delta-ferrite field. This heat treatment ensured that the delta-ferrite grains were large and stable, and due to the high surface diffusion of the delta-ferrite phase, the surface of the sample quickly becomes smooth, leading to improved images. The samples were then cooled to 1350 °C and held for 10 minutes in the austenite single-phase field. The reasoning behind this heat treatment was to promote Widmanstätten ferrite plate formation on subsequent cooling, it being well known that an increase in grain size promotes the development of this morphology.[14] Additionally, having stable grains during solution treatment ensured that the austenite grain boundaries are deeply grooved (due to thermal etching) and therefore the austenite grain boundaries could be easily distinguished, not only in the laser scanning confocal microscope, but also during post-transformation metallographic analysis. Samples were cooled from 1350 °C at a rate of 100 °C/min to a temperature of 700 °C and held isothermally until the phase transformation was complete. The heating and cooling cycle was conducted in an infrared heating furnace under ultra-high-purity argon (>99.9999 pct).

In-situ observations of Widmanstätten ferrite plate growth were conducted in a high-temperature laser-scanning confocal microscope (LSCM). In confocal microscopy, laser light is focused by an objective lens onto the object and the reflected beam is focused onto a photo detector *via* a beam splitter. An image is built up by scanning the focused spot relative to the object, which is then stored in an imaging system for subsequent display. Through the use of a confocal pinhole, only light incident from the focal plane is permitted to pass through to the photo detector. Hence, an extremely thin optical section is created, providing a sharp image at high resolution. Because thermal radiation is also blocked by the confocal pinhole, only the polarized reflection of the high-intensity laser beam reaches the imaging sensor and a sharp image is produced. Magnifications up to 1350 times can be achieved. The laser beam in the system used, a He-Ne laser with a wavelength of 632.8 nm and diameter of 0.5 μm, is reflected and scanned by an acoustic optical deflector in the horizontal direction at a rate of 15.7 kHz and by a galvanomirror in the vertical direction at 60 Hz. Specimens are placed at the focal point of a gold-plated ellipsoidal cavity in an infrared furnace beneath a quartz view port. A 1.5 kW halogen lamp located at the other focal point in the cavity heats the specimen by radiation. The specimen and lamp chambers are separated by quartz glass so that the atmosphere of the specimen chamber can be controlled and the lamp can be air-cooled. The temperature, measured by a thermocouple incorporated in the crucible holder, is displayed on a monitor and simultaneously recorded with the image on videotape at a rate of 30 frames per second. Hard copies of the video frames can be made or they can be subjected to digital video analysis using computer software.

The technique chosen to analyze the orientation relationships between allotriomorphs and Widmanstätten ferrite plates was electron backscatter diffraction (EBSD). In this technique, an electron beam of a scanning electron microscope is scanned over the area of interest and the characteristic diffraction patterns are automatically solved and stored. The resulting information is displayed graphically as an orientation map, with regions of the same color indicating contiguous crystallographic orientation. The orientation map can be quantitatively analyzed using misorientation profiles in which the change in crystallographic orientation along a selected path, typically across an allotriomorph/plate transition, is determined. The resolution of this technique is approximately a 1 deg rotation of the crystallographic lattice. This EBSD analysis was conducted in a Leica Stereoscan (Cambridge, U.K.) 440 scanning electron microscope (SEM) fitted with a Channel 4 EBSD system supplied by HKL Technologies (Mobro, Denmark).

III. RESULTS

A. In-Situ *LSCM Observations*

The sequence of laser-scanning confocal microscope observations shown in Figure 1 refers to the nucleation and growth of Widmanstätten ferrite plates from a ferrite allotriomorph. Shown in Figure 1(a) is an austenite grain boundary on which a ferrite allotriomorph has nucleated and begun to grow. Widmanstätten ferrite plates observed using LSCM are characterised by a bright linear region bounded by dark edges. Two well-developed Widmanstätten ferrite plates, that have impinged laterally, extend from the allotriomorph to the left of the frame. Two further plates have nucleated and have just begun to grow from below the position of the well-established plates. The subsequent development of the Widmanstätten ferrite colony is shown in Figure 1(b), 14 seconds later. A number of regularly spaced ferrite plates, approximately 30 μm apart, are observed to grow in a preferred direction toward the left of the frame.

To better illustrate the initial formation and growth of individual plates, a sequence of four frames in which the initial stages of the formation of three Widmanstätten plates were captured is shown in Figure 2. The allotriomorph has a facetted

Table I. Composition of Alloy (Mass Percent)

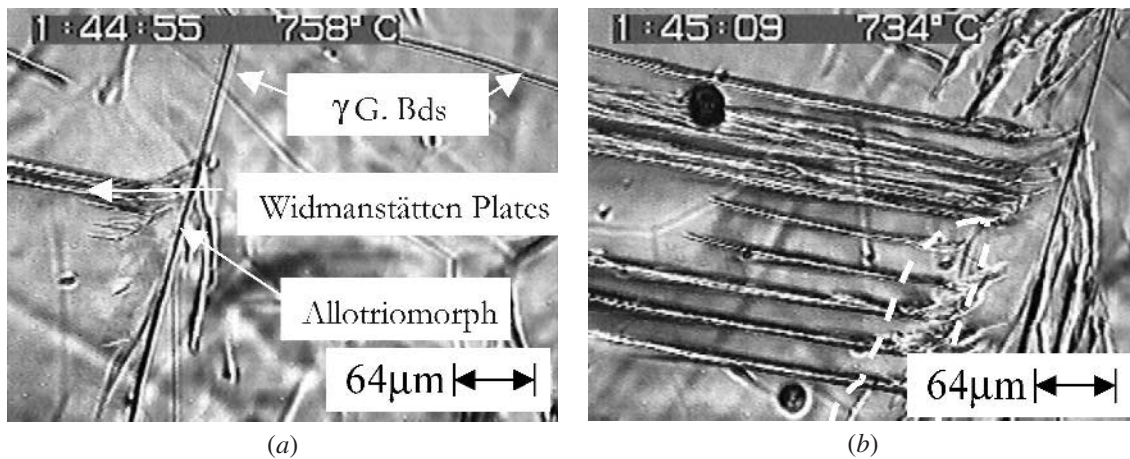| C	P	Mn	Si	Al	S
0.06	0.10	0.4	0.29	<0.005	0.014

Fig. 1—(*a*) and (*b*) Widmanstätten ferrite plates growing from an allotriomorph.
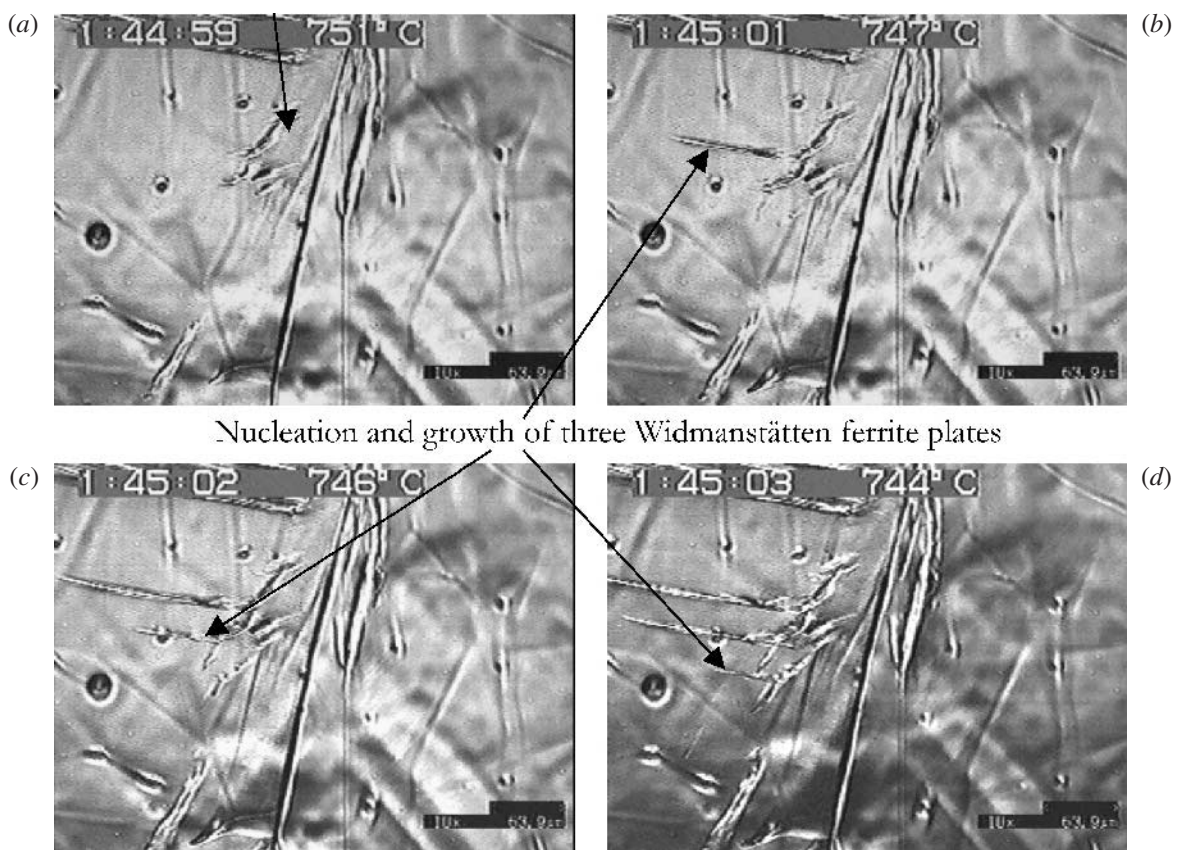

Fig. 2—(*a*) through (*d*) Sympathetic nucleation of Widmanstätten ferrite plates.

appearance, indicating some coherency between the ferrite allotriomorph and the austenite matrix from which it is growing. The three plates appear to grow directly from the stepped regions of the allotriomorph, as would be the case if the plates formed by a process of sympathetic nucleation.

B. *Electron Backscatter Diffraction Analysis*

Although the optical resolution in the confocal microscope is not high enough to discriminate between the nucleation events proposed by the two theories of Widmanstätten ferrite formation, crystallographic orientation analysis can. A direct inference from the unstable interface mechanism is that there should be no misorientation between ferrite allotriomorph and plate, because the Widmanstätten ferrite colony is supposed to be formed as a result of growth and not by a separate nucleation event. The sympathetic nucleation theory, on the other hand, predicts that low-energy boundaries should form between the allotriomorph and nucleating plate, that is, low-angle misorientations should exist. It is generally accepted that low-angle boundaries exhibit misorientations between two crystals of less than 15 deg, and hence, the resolution

of the EBSD technique is sufficient to determine such misorientations experimentally.

Examples of the determination of the crystallographic relationship between Widmanstätten plates and an allotriomorph are presented in Figures 3 and 4. An SEM image showing a Widmanstätten colony and grain boundary allotriomorph is presented in Figure 3. A sample similar to that shown in Figure 1(b) was lightly polished following observation in the LSCM and prepared for SEM analysis. The microstructure shown consists of a prior austenite grain boundary that has been retained due to thermal etching of the free surface. A featureless area, indicating a region of alpha ferrite, has grown from the austenite grain boundary before the formation of Widmanstätten ferrite plates was initiated.

The EBSD analysis presented in Figure 4 clearly indicate that there is a misorientation of about 6 deg between the Widmanstätten ferrite plates and the pre-existing ferrite allotriomorph. This observation is consistent with the prediction that Widmanstätten ferrite plates form by a mechanism of sympathetic nucleation.

In order to illustrate the EBSD analysis performed, the area previously shown in Figure 3 is rotated and reproduced as Figure 4(d). In this image, the positions of the EBSD scans conducted, shown in Figures (a) through (c), respectively, are denoted. A schematic diagram of the area scanned showing the constituent morphology is also included. The graphs of misorientation angle for each scan have been scaled to the maximum angle reported, hence, Figure 4(a) maximum is 0.8 deg, Figure 4(b) maximum is 6 deg, and Figure 4(c) maximum is 55 deg. The first scan, Figure 4(a), profiles normal to the direction of Widmanstätten ferrite plate growth, and stays within the boundaries of the colony. The crystallographic orientation of individual plates within the Widmanstätten colony is uniform with variations of less than 1 deg. This analysis indicates that each plate within the colony has grown with exactly the same orientation, neither confirming nor disproving either of the nucleation mechanisms.

The misorientation profile shown in Figure 4(b) starts in the Widmanstätten colony, runs parallel to the growth direction, and transverses the grain boundary allotriomorph. Within the Widmanstätten colony, there is a high degree of uniformity in crystallographic orientation, as there is in the
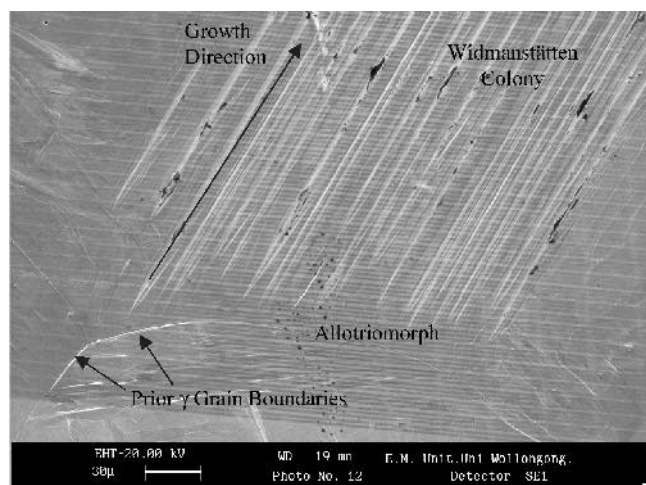
allotriomorph, both exhibiting variations of less than 1 deg. However, there is a 6 deg misorientation between the grain boundary allotriomorph and the Widmanstätten colony. This finding does not support the proposition that Widmanstätten plates can form through the formation of instabilities in the propagating planar alpha-ferrite/austenite growth front. For the Widmanstätten colony to have formed through a mechanism whereby the plates grow from perturbations in the planar interface would require that the plates and allotriomorph be monolithic (with exactly the same crystallographic orientation). Evidently, this is not the case for this particular Widmanstätten colony/allotriomorph combination.

The misorientation profile shown in Figure 4(c) was generated to highlight the change in crystallographic orientation transverse across high-angle grain boundaries. High-angle grain boundaries are those that show a misorientation greater than 15 deg, indicative of regions of the specimen that have formed from separate nucleation events. The scan commences from the top of the EBSD map, running normal to the direction of Widmanstätten ferrite growth, across both edges of the Widmanstätten colony. The position on the map where the profile crosses grain boundaries appears as sharp spikes with a misorientation of 55 and 34 deg, respectively. The misorientation of individual plates within the Widmanstätten colony is less than 1 deg, confirming the results from the initial scan.

Other Widmanstätten colonies that have grown from ferrite allotriomorphs yielded similar results. As an example, EBSD analysis of the specimen shown in Figures 1 and 2 revealed a 9 to 10 deg misorientation between the allotriomorph and the Widmanstätten plates. Hence, *in-situ* observation and crystallographic orientation analysis provide evidence in support of the conclusion that a mechanism of sympathetic nucleation is responsible for the formation and growth of Widmanstätten ferrite plates.

IV. DISCUSSION

A. In-Situ *Results*

The analysis of phenomena as observed at a free surface requires careful consideration and validation, especially when issues of growth orientation play a role. The aim in this study was to probe the nucleation mechanism of Widmanstätten ferrite. To ensure that the events observed in the LSCM experiments are representative of events occurring in the bulk, serial sectioning and optical metallography were used to reveal that allotriomorphs and ferrite plates exhibited intimacy in the bulk as well as on the free surface. Phelan[15] has previously described details of the technique. This study revealed that Widmanstätten ferrite plates observed on the surface have formed in the bulk. For example, Widmanstätten ferrite plates observed on the surface could be followed to a depth of 150 μm by serial sectioning.

The growth of plates of ferrite during austenite decomposition is recognized to occur with a preferred orientation relationship between precipitate and matrix. An example of the implications of such growth for *in-situ* observations is presented in Figure 5(a), where a set of plates growing from the right of the frames strikes an austenite grain boundary and grows into the adjacent austenite grain with a different trajectory (Figure 5(b)). This attendant change in trajectory
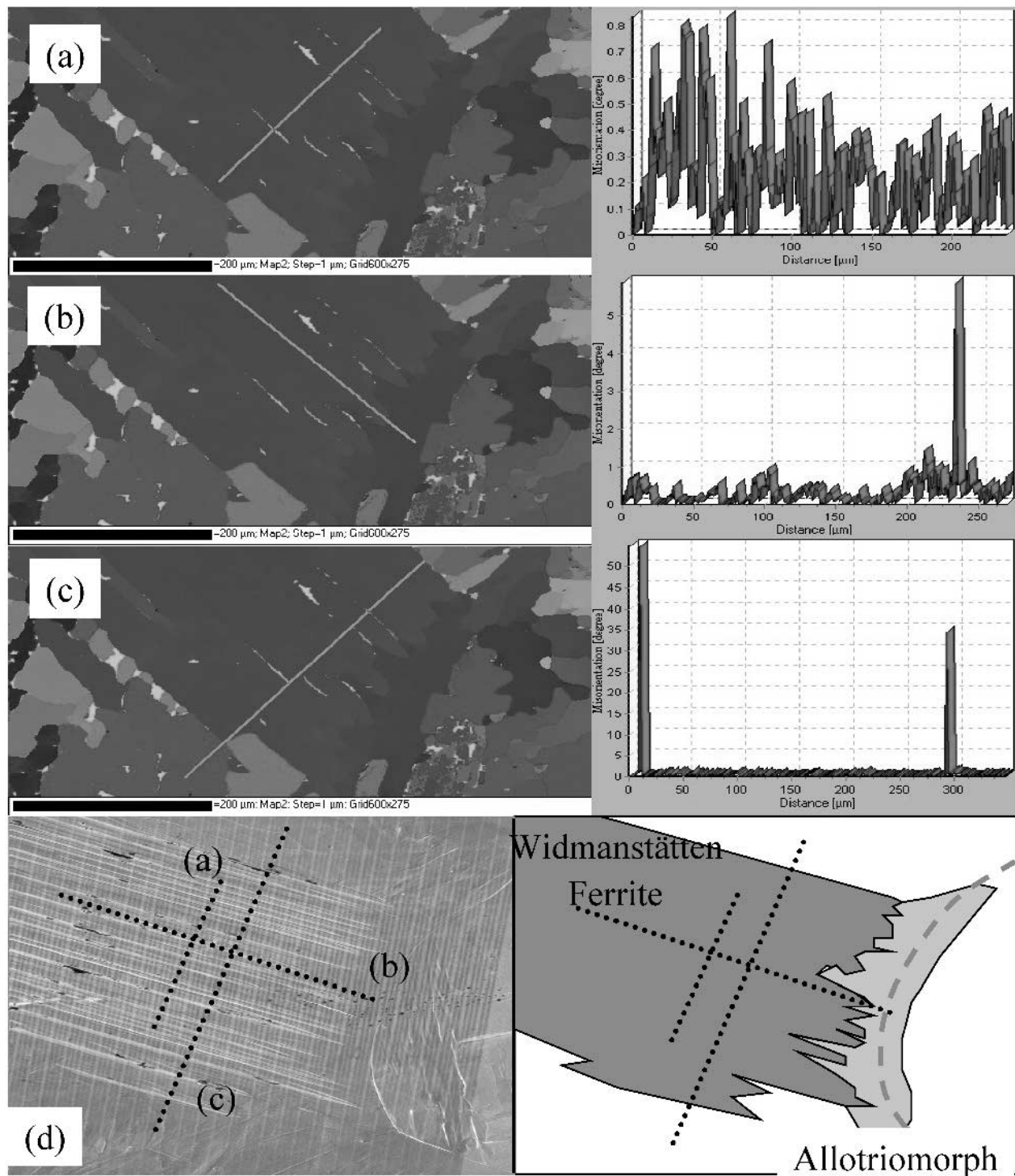

Fig. 3—SEM image of Widmanstätten colony.

Fig. 4—(*a*) through (*d*) EBSD analysis of Widmanstätten ferrite colony.

occurs not only within the plane of view but out of the plane as well. This presents problems for the accurate analysis of growth rates if the growing plates cannot be correctly oriented in three-dimensional space. Of course, this situation is not only of issue with *in-situ* observations made using LSCM, but is also relevant to previous studies into plate growth rates, which have relied upon single sections of the bulk followed by metallographic analysis.

B. *Electron Backscatter Diffraction*

In a prior study, Kral *et al.*[16] measured crystallographic misorientation of cementite plates after etching away the retained austenite matrix. They were aware of the possibility that mechanical bending of the exposed plates could lead to the measured misorientations, and hence, that the misorientations were artifacts and not indicative of sympathetic nucleation. In the present study, unlike that of Kral *et al.,*
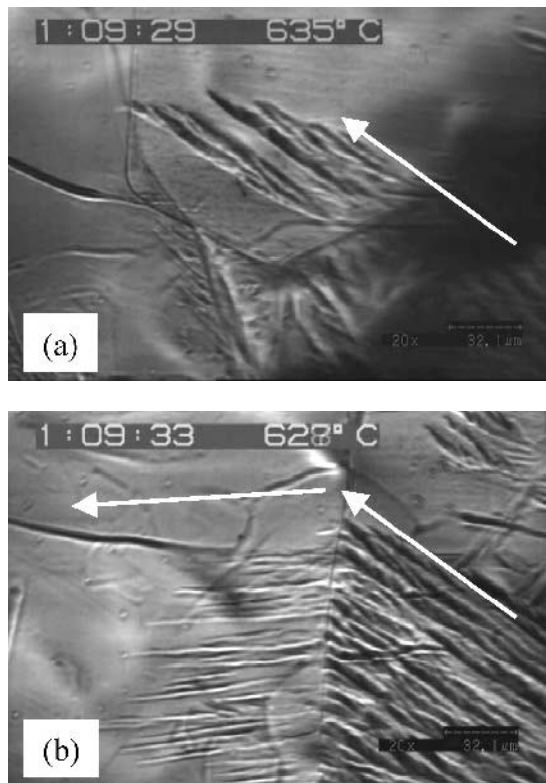
Fig. 5—(*a*) and (*b*) Change in direction of growth and surface relief of ferrite plates across an austenite grain boundary (LSCM).

the decomposition of austinite has proceeded to completion; the matrix has not been stripped away, and therefore, the misorientations observed cannot be the result of plate bending during sample preparation. Hence, the measured crystallographic misorientations cannot be artifacts introduced by polishing.

In conclusion, for a Widmanstätten colony to form by a mechanism where the plates grow from perturbations in a propagating planar interface would require that the plates and allotriomorph be monolithic with contiguous crystallography. *In-situ* observations combined with optical microscopy and EBSD analysis have clearly shown that this is not the case. *In-situ* observation has shown that individual Widmanstätten ferrite plates nucleate on pre-existing ferrite allotriomorphs and growth occurs by the progression of individual plates. Moreover, there is a distinct misorientation between the newly formed colony of Widmanstätten plates and the ferrite allotriomorph on which it formed. These findings provide convincing prima facie evidence that Widmanstätten ferrite plates form by a mechanism of sympathetic nucleation and grow as individual plates.

V. CONCLUSIONS

The combination of *in-situ* observations of Widmanstätten ferrite formation in a low-carbon steel using high-temperature laser scanning confocal microscopy, followed by electron backscatter diffraction analysis of the same area, has proven to be a powerful new experimental approach. New insights have been gained about the decomposition of austenite into Widmanstätten morphology. However, it is important to ensure that the potential influence of the free surface on the *in-situ* observations is duly taken into account.

In-situ observations indicated that the Widmanstätten ferrite plates nucleate on the interface between the austenite parent phase and alpha-ferrite allotriomorphs. Subsequent EBSD analysis has shown that there is a 5 to 10 deg misorientation across the allotriomorph/Widmanstätten interface. These findings provide strong experimental evidence in favor of the sympathetic nucleation mechanism proposed by Aaronson *et al.*[6] The proposal that Widmanstätten ferrite plates originate from instabilities that develop in a growing austenite/ferrite interface,[4] the so-called Mullins–Sekerka type instability, is not supported by the experimental evidence obtained in this study. Both the *in-situ* observations (using LSCM) and crystallographic orientation analysis (using EBSD) support the proposal that sympathetic nucleation is the mechanism by which Widmanstätten ferrite plates nucleate and grow in low-carbon steels.

REFERENCES

1. C.A. Dube, H.I. Aaronson, and R.F. Mehl: *Rev. Met.,* 1958, vol. 55, p. 201.
2. H.I. Aaronson: in *The Decomposition of Austenite by Diffusional Processes,* V.F. Zackay and H.I. Aaronson, eds., Interscience, New York, NY, 1962.
3. D. Dunne: *Mater. Forum,* 1999, vol. 23, pp. 63-76.
4. R.D. Townsend and J.S. Kirkaldy: *Trans. ASM,* 1968, vol. 61, pp. 605-19.
5. J.S. Kirkaldy: *Rep. Progr. Phys.,* 1992, vol. 55, pp. 723-95.
6. H.I. Aaronson, G. Spanos, R.A. Masamura, R.G. Vardiman, D.W. Moon, E.S.K. Menon, and M.G. Hall: *Mater. Sci. Eng.,* 1995, vol. B32, pp. 107-23.
7. W.W. Mullins and R.F. Sekerka: *J. Appl. Phys.,* 1963, vol. 34 (2), pp. 323-29.
8. W.W. Mullins and R.F. Sekerka: *J. Appl. Phys.,* 1964, vol. 35 (2), pp. 444-51.
9. H.I. Aaronson and C. Wells: *Trans. Am. Inst. Mining Eng.,* 1956, vol. 206, p. 1216.
10. P.G. Shewmon: *Trans. TMS-AIME,* 1965, vol. 233, pp. 736-48.
11. E.S.K. Menon and H.I. Aaronsons: *Acta Metall.,* 1987, vol. 35, p. 549.
12. K. Ameyama, G.C. Weatherly, and K.T. Aust: *Acta Metall.,* 1992, vol. 40, pp. 1835-46.
13. G. Spanos and M.G. Hall: *Metall. Mater. Trans. A,* 1996, vol. 27A, pp. 1519-34.
14. P.R. Krahe, K.R. Kinsman, and H.I. Aaronson: *Acta Metall.,* 1972, vol. 20, pp. 1109-21.
15. D.J. Phelan: Ph.D. Thesis, University of Wollongong, Wollongong, 2002.
16. M.V. Kral, M.A. Mangan, G. Spanos, and R.O. Rosenberg: *Mater. Characterization,* 2000, vol. 45 (1), pp. 17-23.